Progress In Electromagnetics Research C, Vol. 10, 111–127, 2009

MIMO ANTENNA MODELLING USING THE EFFECTIVE LENGTH MATRICES

V. Papamichael and C. Soras

Department of Electrical and Computer Engineering
University of Patras
Rio-Patras 26500, Greece

Abstract—A hybrid electromagnetic-network analysis of the antennas-channel multiple input multiple output (MIMO) communication subsystem is presented. The analysis is based on the antenna effective and realized effective length matrices, which relate in a compact mathematical way the radiated and received electric field intensities to the network characteristics of actual and coupled transmitting (Tx) and receiving (Rx) multi-element antenna (MEA) systems. The effective length matrices are calculated via the active power gain and phase antenna patterns obtained by means of any full wave computational electromagnetics (CEM) field solver. It is shown that the realized effective length matrix is suitable for the S-parameter analysis of a MIMO communication link, while the effective length matrix is convenient for its Z-parameter analysis. The effective length matrix framework is applied to a free space 2×2 coupled dipoles MIMO system and its results are in excellent agreement to those obtained by a Method of Moments (MoM) based field solver.

1. INTRODUCTION

The vector effective length of a single element antenna is a well known concept for characterizing both its transmitting (Tx) and receiving (Rx) modes of operation instead of utilizing the radiation patterns [1–3]. It has been applied to various studies including for example wire, slot, printed, mobile phone, RFID and ultra wideband antennas [4–9]. Regarding multi-element antenna (MEA) structures, on the other hand, the effective length concept has recently been used to model only

Corresponding author: C. Soras (soras@ece.upatras.gr).

wire antenna arrays, which in most cases consist of linear dipoles [10–15].

The purpose of this paper is twofold: First, it presents the methodology for determining the effective and realized effective length matrices of an arbitrary actual and coupled MEA configuration at the early design stage by means of any full wave computational electromagnetics (CEM) field solver. These matrices are calculated through the active power gain and phase antenna patterns [16], which can be deduced by simulating the MEA system in its Tx mode of operation. The effective length matrices can be used to model both the Tx and Rx mode of operation of reciprocal as well as non-reciprocal MEA systems. Second, it incorporates the effective length matrices into the radio frequency (RF) transmission chain network models of Multiple Input Multiple Output (MIMO) communication systems operating in multipath wireless channels [17, 18]. The effective length matrices relate in a compact form the radiated and received electric field intensities to the ingoing and outgoing wave vectors at the Tx and Rx antenna ports respectively. It is shown that the realized effective length matrix is useful for the S-parameter analysis of a MIMO communication link, while the effective length matrix is convenient for its Z-parameter analysis.

In Section 2, the hybrid electromagnetic-network analysis of the Tx and Rx modes of a MEA system via the effective length matrices is presented. This analysis is then used in Section 3 to derive the S-parameter and Z-parameter matrices of the MIMO transmission in multipath wireless channels. The proposed framework is applied in Section 4 to a free space 2×2 coupled dipoles MIMO system and its results are compared to those obtained by a Method of Moments (MoM) based computational electromagnetics field solver.

2. HYBRID ELECTROMAGNETIC-NETWORK ANALYSIS OF MEA SYSTEMS

This section begins with a synopsis of the S-parameter representation of the Tx and Rx modes of a coupled MEA system and proceeds with the modeling of a transmitting MEA system via the realized effective length matrix. The response of a receiving MEA system under a uniform plane wave excitation is then determined by applying a reciprocity relationship proved in [19] and the relation between the effective and the realized effective length matrices is derived.

2.1. Network Representation of the Transmitting and Receiving MEA Modes

The Tx and Rx modes of an M-port MEA system are represented under the network theory framework [17, 18] as depicted in Fig. 1. According to the signal flow diagram illustrated in Fig. 2(a), the scalar network quantities involved with the Tx mode of operation are related by

$$\mathbf{a}_T = \mathbf{S}_S \mathbf{b}_T + \mathbf{b}_S \tag{1a}$$

$$\mathbf{b}_T = \mathbf{S}_T \mathbf{a}_T \tag{1b}$$

where $\mathbf{b}_S$ and $\mathbf{S}_S$ are the $M \times 1$ source wave vector and the $M \times M$ S-parameter matrix of the source respectively, $\mathbf{a}_T$ and $\mathbf{b}_T$ are the $M \times 1$ ingoing and outgoing wave vectors at the MEA's input terminals and $\mathbf{S}_T$ is the $M \times M$ S-parameter matrix of the MEA in its Tx mode of operation. Similarly and according to Fig. 2(b), for the Rx mode of operation we have

$$\mathbf{a}_R = \mathbf{S}_R \mathbf{b}_R + \mathbf{b}_E \tag{2a}$$

$$\mathbf{b}_R = \mathbf{S}_L \mathbf{a}_R \tag{2b}$$

where $\mathbf{b}_E$ is the induced by the electric field excitation $M \times 1$ wave vector, $\mathbf{a}_R$ and $\mathbf{b}_R$ are the $M \times 1$ ingoing and outgoing wave vectors at the MEA's termination load, which is characterized by the $M \times M$ S-parameter matrix $\mathbf{S}_L$ and $\mathbf{S}_R$ is the $M \times M$ S-parameter matrix of the MEA in its Rx mode of operation. For a reciprocal MEA system $\mathbf{S}_R = \mathbf{S}_T$, while for a non reciprocal $\mathbf{S}_R = \mathbf{S}_T^T$ where the superscript T denotes the transpose operation [19].

2.2. Transmitting MEA Modeling via the Effective Length Matrix

To proceed with the electromagnetic analysis of the MEA's Tx mode of operation, a spherical coordinate system with its origin O located at the MEA's phase center is defined as shown in Fig. 3. The position vectors $\mathbf{r}' = r'\hat{\boldsymbol{\alpha}}_r'$ and $\mathbf{r} = r\hat{\boldsymbol{\alpha}}_r$ point respectively, to an arbitrary point P' inside the volume V occupied by the antenna and to an observation point P located in the far-field antenna region where the phasor of the radiated electric field is $\mathbf{E}_T(\theta, \phi)$. In order to keep the mathematical expressions compact, in the rest of the paper the (θ, ϕ) dependence will be suppressed but understood.

The vector electromagnetic quantities can be related to the scalar network ones using the realized vector effective length $\boldsymbol{\ell}_{e_m}^r = \ell_{\theta_m}^r \hat{\boldsymbol{\alpha}}_\theta +$

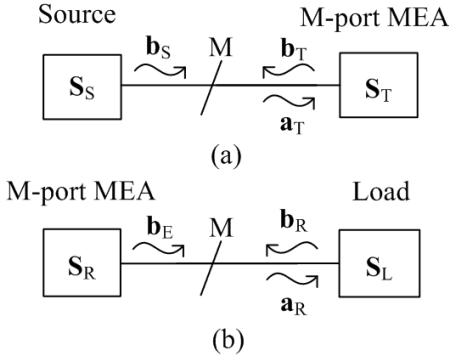

Figure 1. Network representation of an M-port MEA at its (a) Tx and (b) Rx modes of operation.

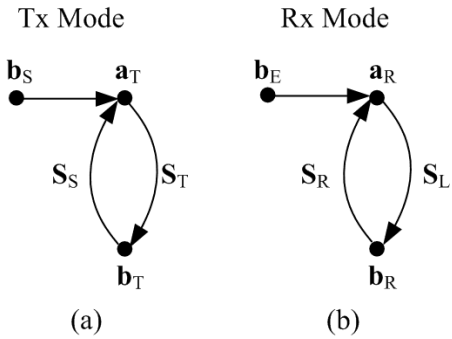

Figure 2. Signal flow diagrams of an M-port MEA at its (a) Tx and (b) Rx modes of operation.

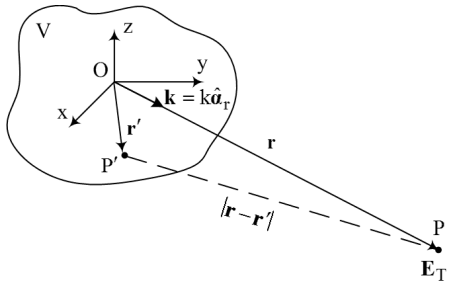

Figure 3. A MEA system at its Tx mode of operation.

$\ell^r_{\phi_m}\hat{\boldsymbol{\alpha}}_\phi$ ($m = 1$ to M), which is defined by

$$\ell^r_{\theta/\phi_m} \triangleq \frac{F_{\theta/\phi_m}}{i^+_{T_m}} \text{ (m)} \tag{3}$$

where the slash "/" stands for "OR", the subscript m denotes that the mth port of the MEA is excited assuming that all antenna ports are terminated to the characteristic impedance of the feeding transmission lines Z_0 (i.e., $\mathbf{S}_S = 0$) and F_{θ/ϕ_m} is the θ/ϕ component of the far-field radiation vector defined through the current density on the MEA structure [2]. In the definition of the realized vector effective length given by (3), two points should be mentioned. First, the ingoing current wave at each port is used instead of the total current, through which the traditional vector effective length $\boldsymbol{\ell}_{e_m} = \ell_{\theta_m}\hat{\boldsymbol{\alpha}}_\theta + \ell_{\phi_m}\hat{\boldsymbol{\alpha}}_\phi$ is defined [1, 2]

$$\ell_{\theta/\phi_m} \triangleq \frac{F_{\theta/\phi_m}}{i_{T_m}} \text{ (m)} \tag{4}$$

Second, given that no backward reflections occur at the source's side ($\mathbf{S}_S = 0$), all the incident wave currents, except the one at the excited port, are zero. In this manner, the realized vector effective length of each antenna element depends only on the ingoing current wave excitation at its port. Consequently, the electric field radiated by a fully excited MEA system will be evaluated by applying the superposition principle using, instead of the total currents, the ingoing current waves as the independent sources.

In order to determine the realized vector effective length $\boldsymbol{\ell}^r_{e_m}$ of each element, the three dimensional active power gain ($\mathbf{G}^a_m$) and phase ($\boldsymbol{\psi}^a_m$) antenna patterns are required, which are defined by

$$G^a_{\theta/\phi_m} \triangleq \frac{4\pi U_{\theta/\phi_m}}{P_{in_m}} \overset{[2]}{=} \frac{\omega\mu_0 k}{8\pi P_{in_m}} \left|F_{\theta/\phi_m}\right|^2 \tag{5a}$$

$$\psi^a_{\theta/\phi_m} \triangleq \arg\left(\frac{F_{\theta/\phi_m}}{i^+_{T_m}}\right) \tag{5b}$$

where ω is the angular frequency, μ_0 the free space magnetic permeability, k the wave number, $\mathbf{U}_m$ the radiation intensity and P_{in_m} the input power in the M-port antenna when only the mth port is excited and $\mathbf{S}_S = 0$ [20]

$$P_{in_m} = \frac{1}{2}\left(\mathbf{a}_T^H\mathbf{a}_T - \mathbf{b}_T^H\mathbf{b}_T\right) = \frac{1}{2}Z_0\left(1 - \sum_{i=1}^{M}\left|S_{m,i}\right|^2\right)\left|i^+_{T_m}\right|^2 \tag{6}$$

where the superscript H denotes the conjugate transpose. It is noted that the active power gain patterns defined in (5a), exclude the impedance mismatches according to the IEEE standard definition [1]. Combining (3), (5) and (6), the θ and ϕ components of $\boldsymbol{\ell}_{e_m}^r$, when only the mth port of the MEA is excited and $\mathbf{S}_S = 0$, is expressed as follows

$$\ell_{\theta/\phi_m}^r = \sqrt{\frac{4\pi Z_0 \left(1 - \sum_{i=1}^{M} |S_{m,i}|^2\right) G_{\theta/\phi_m}^a}{\omega\mu_0 k}} \exp(j\psi_{\theta/\phi_m}^a) \tag{7}$$

In this case, the electric field radiated in the far field region of the MEA can be expressed through [2]

$$E_{T\theta/\phi_m} = -j\omega\mu_0 \frac{\exp(-jkr)}{4\pi r} F_{\theta/\phi_m} \tag{8}$$

Using (3) and $a_{T_m} = i_{T_m}^+ \sqrt{Z_0}$ [20] in (8) it follows that

$$E_{T\theta/\phi_m} = -\frac{j\omega\mu_0}{\sqrt{Z_0}} \frac{\exp(-jkr)}{4\pi r} \ell_{\theta/\phi_m}^r a_{T_m} \tag{9}$$

The electric field $\mathbf{E}_T$ radiated by a fully excited MEA is then derived by applying the superposition principle, using the ingoing waves at the antenna's ports as the independent sources

$$\mathbf{E}_T = -\frac{j\omega\mu_0}{\sqrt{Z_0}} \frac{\exp(-jkr)}{4\pi r} \mathbf{L}_e^{rT} \mathbf{a}_T \tag{10}$$

where $\mathbf{L}_e^r$ is the realized effective length matrix, defined by

$$\mathbf{L}_e^r \triangleq \begin{bmatrix} \ell_{\theta_1}^r & \ell_{\theta_2}^r & \cdots & \ell_{\theta_M}^r \\ \ell_{\phi_1}^r & \ell_{\phi_2}^r & \cdots & \ell_{\phi_M}^r \end{bmatrix}^T \text{(m)} \tag{11}$$

As implied by (10), at the Tx mode of operation $\mathbf{L}_e^r$ relates $\mathbf{a}_T$ to $\mathbf{E}_T$ in a convenient mathematical way. In the next sub-section we will derive the corresponding relationship for the Rx mode.

2.3. Receiving MEA Modeling under a Uniform Plane Wave Excitation

In order to determine the response of an Rx MEA, consider now that the same M-port antenna system of the previous sub-section is excited by a uniform plane wave (Fig. 4). The origin of the spherical coordinate

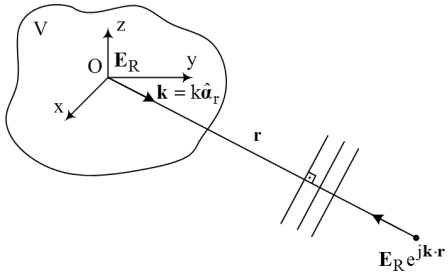

Figure 4. The MEA system of Fig. 3 excited by an incident uniform plane wave.

system is again placed at the phase center of the MEA, where the phasor of the incident electric field intensity is $\mathbf{E}_R$.

The derivation of the wave vector $\mathbf{b}_E$ induced by the electric field excitation $\mathbf{E}_R$ is based on the electromagnetic analysis of MEA systems presented in [19], where it has been proved by means of the Lorentz's reciprocity theorem that the Tx and Rx modes of operation are connected through the following relationship

$$\mathbf{v}_T^T \mathbf{i}_R + \mathbf{i}_T^T \mathbf{v}_R = -\left(j\omega\mu_0\right)^{-1} \frac{4\pi r}{\exp\left(-jkr\right)} \mathbf{E}_T^T \mathbf{E}_R \tag{12}$$

where the electric field intensities $\mathbf{E}_R$ and $\mathbf{E}_T$ are calculated in the same θ, ϕ direction. The voltage and current vectors are related to the ingoing and outgoing wave vectors through the following well known relationships [20]

$$\mathbf{v}_T = \sqrt{Z_0}\left(\mathbf{I} + \mathbf{S}_T\right)\mathbf{a}_T \tag{13a}$$

$$\mathbf{i}_T = \frac{1}{\sqrt{Z_0}}\left(\mathbf{I} - \mathbf{S}_T\right)\mathbf{a}_T \tag{13b}$$

$$\mathbf{v}_R = \sqrt{Z_0}\left(\mathbf{I} + \mathbf{S}_L\right)\mathbf{a}_R \tag{14a}$$

$$\mathbf{i}_R = \frac{1}{\sqrt{Z_0}}\left(\mathbf{I} - \mathbf{S}_L\right)\mathbf{a}_R \tag{14b}$$

where $\mathbf{I}$ is the $M \times M$ identity matrix. Substituting (13), (14) and (10) into (12), it follows that

$$\mathbf{b}_E = \frac{1}{2\sqrt{Z_0}} \mathbf{L}_e^r \mathbf{E}_R \tag{15}$$

which is the compact expression that relates the Rx mode parameters $\mathbf{b}_E$ and $\mathbf{E}_R$ through the realized effective length matrix $\mathbf{L}_e^r$.

2.4. Relationship between the Two Effective Length Matrices

Combining (2a) and (14a) under the assumption of an open-circuit terminated Rx MEA (i.e., $\mathbf{S}_L = \mathbf{I}$ and $\mathbf{v}_R = \mathbf{v}_{oc}$) it follows that

$$\mathbf{b}_E = \frac{1}{2\sqrt{Z_0}} \left(\mathbf{I} - \mathbf{S}_R\right) \mathbf{v}_{oc} \tag{16}$$

Equating the right hand sides of (15) and (16) and solving for the open-circuit Rx voltage vector $\mathbf{v}_{oc}$ results to

$$\mathbf{v}_{oc} = \left(\mathbf{I} - \mathbf{S}_R\right)^{-1} \mathbf{L}_e^r \mathbf{E}_R \tag{17}$$

which by comparison with [11]

$$\mathbf{v}_{oc} = \mathbf{L}_e \mathbf{E}_R \tag{18}$$

determines the mathematical relationship between the effective length matrix $\mathbf{L}_e$ and the realized effective length matrix

$$\mathbf{L}_e^r = \left(\mathbf{I} - \mathbf{S}_R\right) \mathbf{L}_e \tag{19}$$

This equation implies that $\mathbf{L}_e^r$ is a linear transformation of $\mathbf{L}_e$ and vice versa. For single antenna elements, the simplified version of (19) has already been utilized in [9], but was not generalized for the case of coupled MEA systems. (15) and thus $\mathbf{L}_e^r$, will be useful for the S-parameter analysis of a MIMO communication link, while (18) and thus $\mathbf{L}_e$, will be convenient for the Z-parameter analysis.

3. MIMO SYSTEM MODELLING IN MULTIPATH WIRELESS CHANNELS

3.1. S-parameter Analysis

The network representation of an $N \times M$ MIMO system comprising an M-port transmitting (Tx) antenna and an N-port receiving (Rx) antenna is depicted in Fig. 5. From the signal flow diagram of the MIMO system shown in Fig. 6, the wave vectors $\mathbf{a}_T$, $\mathbf{a}_R$, $\mathbf{b}_T$ and $\mathbf{b}_R$ are related through the MIMO network S-parameter matrix $\mathbf{S}_H$ as follows [17, 18]

$$\begin{bmatrix} \mathbf{b}_T \\ \mathbf{a}_R \end{bmatrix} = \underbrace{\begin{bmatrix} \mathbf{S}_{TT} & \mathbf{S}_{TR} \\ \mathbf{S}_{RT} & \mathbf{S}_{RR} \end{bmatrix}}_{\mathbf{S}_H} \begin{bmatrix} \mathbf{a}_T \\ \mathbf{b}_R \end{bmatrix} \tag{20}$$

where $\mathbf{S}_{RT}$ and its reciprocal $\mathbf{S}_{TR}$ are the S-parameter matrices which characterize the MIMO transmission, $\mathbf{S}_{TT}$ is the S-parameter matrix of the Tx MEA in its Tx mode of operation and $\mathbf{S}_{RR}$ the S-parameter matrix of the Rx MEA in its Rx mode of operation.

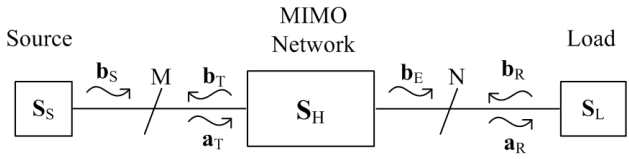

Figure 5. Network representation of a MIMO wireless communication system.

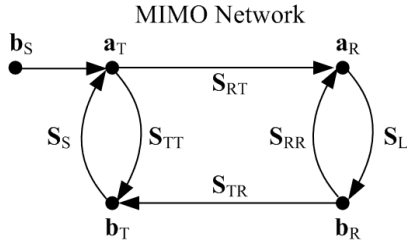

Figure 6. Signal flow graph of a MIMO wireless communication system.

According to (20), the ingoing to the load wave vector $\mathbf{a}_R$ is given by

$$\mathbf{a}_R = \mathbf{S}_{RR}\mathbf{b}_R + \mathbf{S}_{RT}\mathbf{a}_T \tag{21}$$

Comparing (21) to (2a), which holds for the MEA system's Rx mode of operation, the wave vector $\mathbf{b}_E$ induced by the electric field excitation can be expressed through

$$\mathbf{b}_E = \mathbf{S}_{RT}\mathbf{a}_T \tag{22}$$

In order to estimate $\mathbf{S}_{RT}$ in a multipath wireless channel consider a snapshot of the wireless channel and its L depolarization matrices which include the various possible depolarization mechanisms present at each path. The L 2×2 depolarization matrices, which alter the amplitude, phase and polarization of the electric fields [21], incorporate in addition the path losses due to the distance travelled by the wave and are mathematically expressed by

$$\mathbf{D}_l = \begin{bmatrix} D_{l,\theta\theta} & D_{l,\theta\phi} \\ D_{l,\phi\theta} & D_{l,\phi\phi} \end{bmatrix}, \; l = 1 \ldots L \tag{23}$$

By taking into account only the lth multipath component, the electric field at the Rx MEA due to a fully excited Tx MEA can be expressed using (10) by substituting the free-space spherical spreading factor $1/4\pi r$ with the depolarization matrix $\mathbf{D}_l$

$$\mathbf{E}_{R,l} = -\frac{j\omega\mu_0}{\sqrt{Z_0}} \exp\left(-jkr_l\right) \mathbf{D}_l \left(\mathbf{L}_{e,T}^r\right)^T \mathbf{a}_T \tag{24}$$

where r_l is the total length of the lth path. The induced wave $\mathbf{b}_E$ for this case is given by substituting (24) into (15) and further applying the superposition principle

$$\mathbf{b}_E = -\frac{j\omega\mu_0}{2Z_0} \sum_{l=1}^{L} \exp\left(-jkr_l\right) \mathbf{L}_{e,R}^r \mathbf{D}_l \left(\mathbf{L}_{e,T}^r\right)^T \mathbf{a}_T \tag{25}$$

Comparing (25) with (22), it follows that $\mathbf{S}_{RT}$ for a multipath wireless channel can be expressed by

$$\mathbf{S}_{RT} = -\frac{j\omega\mu_0}{2Z_0} \sum_{l=1}^{L} \exp\left(-jkr_l\right) \mathbf{L}_{e,R}^r \mathbf{D}_l \left(\mathbf{L}_{e,T}^r\right)^T \tag{26}$$

This equation implies that the utilization of the Tx and Rx realized effective length matrices results in a compact formulation of the $\mathbf{S}_{RT}$ matrix in contrast to [17, Eq. (28)]. As far as the evaluation of all the snapshots of the $\mathbf{D}_l$ matrix in a multipath channel is concerned, this is beyond the scope of this work and can be accomplished using either deterministic (ray-tracing) or stochastic (geometry-based or non-geometrical) modeling approaches [22].

3.2. Z-parameter Analysis

If a Z-parameters analysis of a MIMO system is desired, the utilization of the effective length matrix $\mathbf{L}_e$ is more convenient than $\mathbf{L}_e^r$. Based on their relationship (19) and using additionally (13b) and (16) in (25) it follows that

$$\mathbf{v}_{oc} = -j\omega\mu_0 \sum_{l=1}^{L} \exp\left(-jkr_l\right) \mathbf{L}_{e,R} \mathbf{D}_l \left(\mathbf{L}_{e,T}\right)^T \mathbf{i}_T \tag{27}$$

Since the MIMO transmission Z-parameter matrix $\mathbf{Z}_{RT}$ is defined through $\mathbf{v}_{oc} = \mathbf{Z}_{RT}\mathbf{i}_T$ [18], it can be obtained from (27) as

$$\mathbf{Z}_{RT} = -j\omega\mu_0 \sum_{l=1}^{L} \exp\left(-jkr_l\right) \mathbf{L}_{e,R} \mathbf{D}_l \left(\mathbf{L}_{e,T}\right)^T \tag{28}$$

The corresponding to (28) mathematical formula that uses the radiation and reception antenna patterns has been given in [18, Eq. (37)]. By substituting (19) and (28) into (26), the following relationship between $\mathbf{S}_{RT}$ and $\mathbf{Z}_{RT}$ is obtained

$$\mathbf{S}_{RT} = (\mathbf{I} - \mathbf{S}_{RR}) \frac{\mathbf{Z}_{RT}}{2Z_0} (\mathbf{I} - \mathbf{S}_{TT}) \tag{29}$$

4. EXAMPLE: A 2×2 COUPLED DIPOLES MIMO SYSTEM IN FREE SPACE

As an example of the framework presented in the previous sections, the S-parameter transmission matrix $\mathbf{S}_{RT}$ of a MIMO system comprising two pairs of coupled dipole antennas operating in free space at the 5.2 GHz ISM band (5.15–5.35 GHz) is calculated (Fig. 7). The length and the radius of the dipoles are $L_d = 0.47\lambda_c$ and $\alpha_d = L_d/200$ respectively, where λ_c is the wavelength of the central frequency of the band (5.25 GHz). The separation distance between the Tx and Rx dipole pairs is $r = 100\lambda_c$ and the inter-element distance is $0.1\lambda_c$. Each pair thus resides in the far-field region of the other and the dipole antennas of each pair exhibit strong mutual coupling.

For free space transmissions $\mathbf{D}$ is simply the free-space spherical spreading factor $1/4\pi r$ and thus (26) and (28) are simplified to the following relationships

$$\mathbf{S}_{RT} = -\frac{j\omega\mu_0}{Z_0} \frac{\exp(-jkr)}{8\pi r} \mathbf{L}^r_{e,R} \left(\mathbf{L}^r_{e,T}\right)^T \tag{30}$$

$$\mathbf{Z}_{RT} = -j\omega\mu_0 \frac{\exp(-jkr)}{4\pi r} \mathbf{L}_{e,R} \left(\mathbf{L}_{e,T}\right)^T \tag{31}$$

which provides a complete model for free space MIMO communication links in contrast to the well known Friis formula which hides the phase information and applies only for SISO links. The realized effective length matrices of the Tx and Rx dipole pairs are computed via the active power gain and phase antenna patterns obtained from a commercial MoM based field solver [23] for eleven equally spaced frequencies inside the 5.2 GHz band. Given that the same dipole antennas are used at both sides of the link, the Tx and Rx realized effective length matrices for each frequency are the same. For example, the realized effective length matrices at the central frequency of the band (5.25 GHz) are

$$\mathbf{L}^r_{e,T}(90^\circ, 0^\circ) = \mathbf{L}^r_{e,R}(90^\circ, 180^\circ) = \begin{bmatrix} 9.513e^{j83.4^\circ} & 0 \\ 9.513e^{j83.4^\circ} & 0 \end{bmatrix} \text{ (mm)} \tag{32}$$

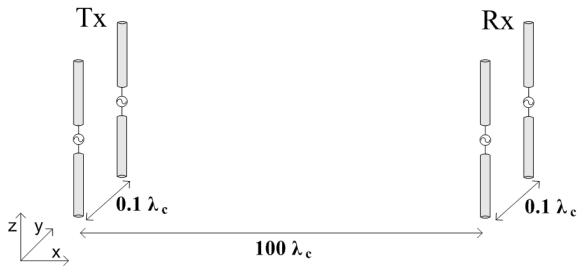

Figure 7. A 2×2 coupled dipoles MIMO antennas operating in free space.

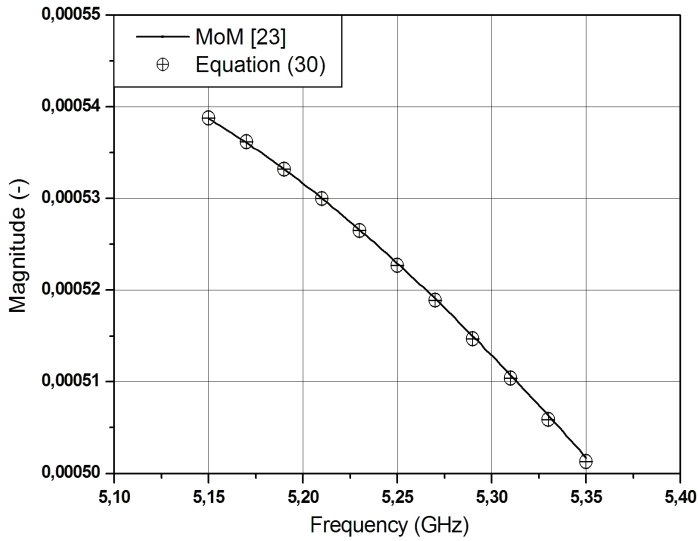

Figure 8. The magnitude of the MIMO transmission S-parameter matrix's elements versus frequency.

where due to the symmetry of Fig. 7, their values are equal for the angles of departure and arrival i.e., $(90°, 0°)$ and $(90°, 180°)$ respectively. Using (19), the corresponding effective length matrices can be also evaluated

$$\mathbf{L}_{e,T}\,(90°, 0°) = \mathbf{L}_{e,R}\,(90°, 180°) = \begin{bmatrix} 18.136e^{j80.5°} & 0 \\ 18.136e^{j80.5°} & 0 \end{bmatrix} \text{ (mm)} \quad (33)$$

These values have been calculated with the phase reference point located on the symmetry axis of the Tx pair at a distance 0.5 mm

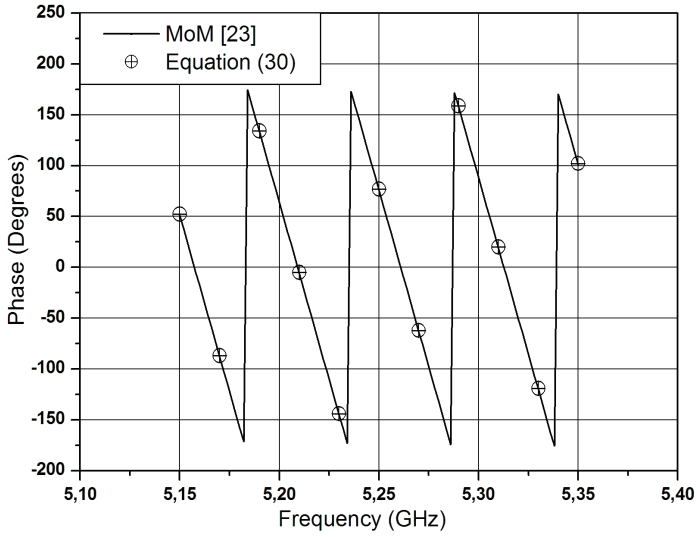

Figure 9. The phase of the MIMO transmission S-parameter matrix's elements versus frequency.

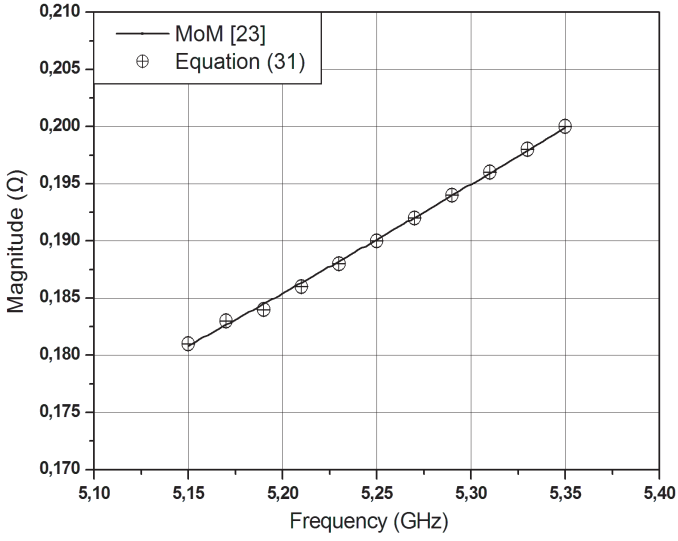

Figure 10. The magnitude of the MIMO transmission Z-parameter matrix's elements versus frequency.

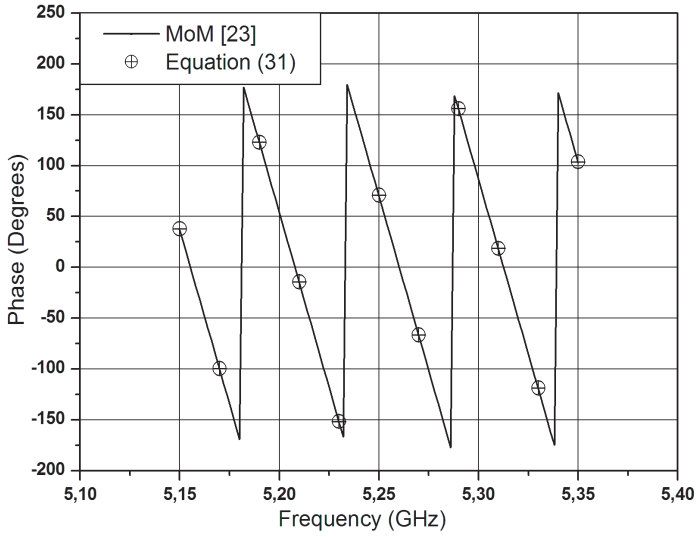

Figure 11. The phase of the MIMO transmission Z-parameter matrix's elements versus frequency.

below the lower ends of the dipoles. The choice of the phase reference point affects the values of the effective length matrices' elements but not those of the $\mathbf{S}_{RT}$ and $\mathbf{Z}_{RT}$ matrices which due to the symmetry of this example are all equal to $5.22 \cdot 10^{-4} e^{j76.9^\circ}$ and $0.19 \cdot e^{j70.9^\circ}$ at 5.25 GHz respectively.

The computed through (30) and (31) magnitude and phase of the $\mathbf{S}_{RT}$ and $\mathbf{Z}_{RT}$ matrices' elements for the whole 5.2 GHz ISM band are in excellent agreement with those obtained via the MoM simulation as illustrated in Figs. 8–11 respectively. A remarkable note is the 0.63 dB and 0.88 dB difference in the magnitude of the $\mathbf{S}_{RT}$ and $\mathbf{Z}_{RT}$ respectively between the upper and lower frequency limits of the band. Another note is that, with increasing frequency, the vector effective lengths of the antennas increase while the realized vector effective lengths decrease.

5. CONCLUSION

Any actual, reciprocal or non-reciprocal, coupled multi-element antenna (MEA) system can be thoroughly represented at both its transmitting (Tx) and receiving (Rx) modes of operation via the effective and realized effective length matrices. The mathematical

relationship between these matrices and the procedure to evaluate them by means of the active power gain and phase patterns obtained by any full wave computational electromagnetics field solver has been presented. The advantage of using these matrices, instead of the traditional radiation patterns, lies in their ability to relate rigorously and compactly the radiated/received electric field intensities to the network characteristics of the Tx/Rx MEA systems. A hybrid electromagnetic-network framework for modelling the combined MEA/channel MIMO subsystem via the effective length matrices under both an S-parameter and a Z-parameter analysis was also developed. As an example of the proposed framework, a 2×2 coupled dipoles MIMO antenna system operating in free space at the 5.2 GHz ISM band was analyzed. The evaluated magnitude and phase of the elements of the S and Z-parameter MIMO transmission matrices were found to be in excellent agreement to those obtained by using a Method of Moments based electromagnetic field solver.

REFERENCES

1. Balanis, C. A., *Antenna Theory: Analysis and Design*, 3rd edition, John Wiley, New York, 2005.
2. Orphanidis, S. J., *Electromagnetic Waves and Antennas*, February 2008. [Online] Available: http://www.ece.rutgers.edu/∼orfanidi-/ewa.
3. Meys, R., "A summary of the transmitting and receiving properties of antennas," *IEEE Antennas and Propagation Magazine*, Vol. 42, No. 3, 49–53, June 2000.
4. Wunsch, A. D. and S.-P. Hu, "A closed-form expression for the driving-point impedance of the small inverted L antenna," *IEEE Transactions on Antennas and Propagation*, Vol. 44, No. 2, 236–242, February 1996.
5. Wunsch, A. D., "The vector effective length of slot antennas," *IEEE Transactions on Antennas and Propagation*, Vol. 39, No. 5, 705–709, May 1991. (comments by R. E. Collin and reply in *IEEE Transactions on Antennas and Propagation*, Vol. 41, No. 3, 389–391, March 1993).
6. Yoon, I.-J., E. Balzovsky, Y. Buyanov, S.-H. Park, Y. Kim, and V. Koshelev, "Active integrated antenna for mobile TV signal reception," *Microwave and Optical Technology Letters*, Vol. 49, No. 12, 2998–3001, December 2007.
7. Nakagawa, Y., M. Mimura, K. Miyano, Y. Koyanagi, and K. Fujimoto, "Improved method for evaluating antenna performance in

mobile environment with consideration of polarization and phase," *IEEE Transactions on Vehicular Technology*, Vol. 52, No. 5, 1189–1195, September 2003.

8. Fuschini, F., C. Piersanti, F. Paolazzi, and G. Falciasecca, "Analytical approach to the backscattering from UHF RFID transponder," *IEEE Antennas and Wireless Propagation Letters*, Vol. 7, 33–35, 2008.
9. Licul, S. and W. Davis, "Unified frequency and time-domain antenna modeling and characterization," *IEEE Transactions on Antennas and Propagation*, Vol. 53, No. 9, 2882–2888, September 2005.
10. Iigusa, K., T. Ohira, and B. Komiyama, "An equivalent weight vector model of array antennas considering current distribution along dipole elements," *Electronics and Communications in Japan, Part 1*, Vol. 89, No. 2, 22–35, February 2006.
11. Kislinasky, A., R. Shavit, and J. Tabrikian, "Direction of arrival estimation in the presence of noise coupling in antenna arrays," *IEEE Transactions on Antennas and Propagation*, Vol. 55, No. 7, 1940–1947, July 2007.
12. Elnaggar, M. S., S. Safavi-Naeini, and S. K. Chaudhuri, "Simulation of the achievable indoor MIMO capacity by using an adaptive phased-array," *Proceedings of the IEEE Radio and Wireless Conference (RAWCON 2004)*, 155–158, Atlanta, GA, September 19–22, 2004.
13. Getu, B. N. and R. Janaswamy, "The effect of mutual coupling on the capacity of the MIMO cube," *IEEE Antennas and Wireless Propagation Letters*, Vol. 4, 240–244, 2005.
14. Farkasvolgyi, A. and L. Nagy, "Mutual coupling effects on the mean capacity of MIMO antenna systems," *PIERS Proceedings*, 103–106, Prague, August 27–30, 2007.
15. Geyi, W., "Multi-antenna information theory," *Progress In Electromagnetics Research*, PIER 75, 11–50, 2007.
16. Kelley, D. F. and W. L. Stutzman, "Array antenna pattern modeling methods that include mutual coupling effects," *IEEE Transactions on Antennas and Propagation*, Vol. 41, No. 12, 1625–1632, December 1993.
17. Waldschmidt, C., S. Schulteis, and W. Wiesbeck, "Complete RF system model for analysis of compact MIMO arrays," *IEEE Transactions on Vehicular Technology*, Vol. 53, No. 3, 579–586, May 2004.
18. Wallace, J. W. and M. A. Jensen, "Mutual coupling in MIMO

wireless systems: A rigorous network theory analysis," *IEEE Transactions on Wireless Communications*, Vol. 3, No. 4, 1317–1325, July 2004.

19. De Hoop, A. T., "The N-port receiving antenna and its equivalent electrical network," *Philips Research Reports*, Vol. 30, 302–315, 1975.
20. Pozar, D. M., *Microwave Engineering*, Addison-Wesley Publishing Company, Inc., USA, 1993.
21. Stutzman, W. L., *Polarization in Electromagnetic Systems*, Artech House, Inc., Norwood, MA, USA, 1992.
22. Almers, P., E. Bonek, A. Burr, N. Czink, M. Debbah, V. Degli-Esposti, H. Hofstetter, P. Kyosti, D. Laurenson, G. Matz, A. F. Molish, C. Oestges, and H. Ozcelik, "Survey of channel and radio propagation models for wireless MIMO systems," *EURASIP Journal on Wireless Communications and Networking*, Vol. 2007, Article ID 19070, doi:10.1155/2007/19070, 2007.
23. Zeland Software Inc., IE3D, http://www.zeland.com.